https://jksus.org

ScientificScholar®
Knowledge is power
Publisher of Scientific Journals

Journal of King Saud University – Science

2025 37 (1) 552024

Original Article

Charge-density analysis of magnesium-doped bentonite: Enhanced structural and electrical properties with tight-binding calculations

Abdulaziz Almalki[a], Talat H Habeeb[b], Hussam Y. Alharbi[c], Ali H. Bashal[c,*]

[a]Department of Physics, Taibah University, Yanbu, Saudi Arabia
[b]Department of Biology, Taibah University, Yanbu, Saudi Arabia
[c]Department of Chemistry, Taibah University, Yanbu, Saudi Arabia

ARTICLE INFO

Keywords:
Charge density analysis
Conductivity
DFT
Dielectric constant
Electric modulus
Homo-Lumo
Magnesium-doped bentonite
Maxwell–Wagner effect

ABSTRACT

This study examines the dielectric properties and structural characteristics of magnesium-doped bentonite (Mg/Bento) composites. The aim was to assess how Mg nanoclusters affect the dielectric behavior and structural changes of bentonite. We prepared the composites using granular bentonite with a surface area of approximately 1000 m/g and magnesium nitrate. X-ray diffraction (XRD) analysis confirmed the presence of SiO_2, quartz, and montmorillonite in both pure and Mg-doped samples, with distinct peaks at 2θ values of 21.52° for SiO_2 and 26.72° for quartz, while Mg-specific peaks appeared at 2θ = 30.16°, 32.56°, and 36.11°, affirming Mg incorporation. Additional impurity phases were noted at 2θ = 39.76° and 47.39°. The calculated lattice parameters for Mg were 2.71 Å and 5.50 Å, with grain sizes of 7 nm for pure bentonite and 15 nm for Mg/Bento. Scanning electron microscopy (SEM) images revealed altered morphologies in Mg/Bento, showing agglomerations and layered structures. Elemental composition analysis via energy dispersive X-ray (EDX) confirmed the presence of Mg, O, Si, Al, and trace elements like Ca and Fe, with notable Mg peaks highlighting the successful incorporation of magnesium into the composite. Dielectric measurements revealed a decrease in permittivity with increasing frequency and a significant increase at higher temperatures for Mg/Bento, attributed to Maxwell-Wagner interfacial charge effects. Tight-binding calculations further revealed charge accumulation at the Mg/bentonite interface and a narrowed highest occupied molecular orbital and lowest unoccupied molecular orbital (HOMO-LUMO) energy gap from 1.6260 eV in pure bentonite to 0.4312 eV in Mg/Bento, indicating enhanced conductivity and electronic properties. These findings demonstrate that incorporating Mg into bentonite affects both its structural and electronic properties, leading to improved dielectric performance.

1. Introduction

Montmorillonite, an aluminum hydro-silicate, is primarily composed of Bentonite (Bento), a clay mineral with a layered structure of two SiO tetrahedral sheets surrounding an Al (OOH) octahedral sheet. This distinctive structure provides bentonite with notable flexibility, thermal stability, and natural acidity, making it suitable for a range of applications (Borah et al., 2022). The introduction of various cations or anions can alter the physical and chemical properties of bentonite, modifying the interlayer gap between the SiO_4 tetrahedral sheets. The modifications significantly influence its electrical characteristics, dielectric properties, and swelling behavior (Neelamma et al., 2022). The incorporation of metal ions into bentonite matrices enhances its catalytic effectiveness and adsorption properties, making it particularly advantageous for environmental applications, such as the removal of heavy metal ions from wastewater (Mutahir et al., 2023). This study focuses on the influence of magnesium (Mg) incorporation on the physical and chemical properties of bentonite, a topic of considerable practical relevance. Magnesium was selected due to its cost-effectiveness, widespread availability, and appropriate ionic radius, which facilitates its incorporation into the bentonite matrix with minimal structural disruption. Additionally, Mg ions exhibit strong coordination properties that can significantly enhance the thermal and dielectric characteristics of bentonite, positioning it as a superior candidate compared to other metals for specific applications. The inherent structure of bentonite also offers opportunities for tailoring its dielectric properties by forming composites with metals, metal oxides, polymers, and other materials (Prasad et al., 2022). The development of nano-scale composites has attracted considerable interest due to their unique physicochemical properties, offering potential advantages in various fields, including chemistry, physics, and biology (Sekunowo et al. 2015). The incorporation of metals or metal oxides into bentonite can significantly enhance its dielectric properties (Bashal, 2024). Studies have shown that incorporating metal ions like Cu^{2+} and Ni^{2+}, as well as metal oxides, can enhance the dielectric strength, increase the dielectric constant, and reduce dielectric loss in bentonite-based composites, thereby improving their overall performance and making them more suitable for applications in capacitors and other electronic devices (Alotaibi et al., 2020; Abou Elfadl et al., 2022; Bashal et al., 2020; Zaki et al., 2023). The wet impregnation method is a highly

***Corresponding author:**
E-mail address: Abishil@taibahu.edu.sa (A. Bashal)

Received: 22 September, 2024 **Accepted:** 27 January, 2025 **Epub Ahead of Print:** 18 March, 2025 **Published:** 22 March, 2025

DOI: 10.25259/JKSUS_55_2024

effective and commonly employed technique for incorporating metal ions into diverse matrices.

This method facilitates an even distribution of metal ions within the material, guaranteeing uniform alterations in dielectric and conductive characteristics throughout the composite. The benefits of the wet impregnation method render it especially advantageous for developing advanced materials that possess customized electrical properties (Jiang, 2006; Mehrabadi et al., 2017). Conversely, the observed enhancements in bentonite composites result from forming new charge transport pathways and alterations in the clay's interlayer spaces, which improve the alignment and distribution of the electric field throughout the material. The advancement of energy storage materials, especially capacitor materials characterized by high dielectric constants and minimal dielectric loss, is a vital area of ongoing investigation for enhancing energy storage efficiency. Although advancements have been made, a gap persists in the existing literature concerning the effects of integrating rare metals, on the dielectric properties of bentonite, underscoring the necessity for additional investigation.

This research explores a magnesium-doped bentonite composite synthesized via a wet impregnation method, examining its structural, dielectric, and electronic properties. The innovative aspects of this study include (1) employing charge-density analysis to investigate interfacial charge accumulation between Mg nanoclusters and bentonite, (2) conducting tight-binding calculations that reveal a reduced highest occupied molecular orbital and lowest unoccupied molecular orbital (HOMO-LUMO) energy gap, enhancing conductivity, and (3) demonstrating Magnesium's role in increasing permittivity and interfacial polarization at elevated temperatures, attributed to the Maxwell-Wagner effect. These enhancements are associated with forming new charge transport pathways and modifications in bentonite's interlayer spaces, which improve the alignment and distribution of the electric field within the material. As advanced energy storage materials, particularly those with high dielectric constants and low dielectric loss, are critical for efficient storage, this study provides a fresh perspective on bentonite functionalization for electronic and energy storage applications, addressing gaps in the existing literature on the impact of rare metals on bentonite's dielectric properties.

2. Experimental

2.1 Materials and methods

This investigation used the materials as received. All reagent operations were performed in a fume chamber.

Granular Bento (CAS# 1302-78-9) from Sigma-Aldrich has a nearly homogeneous particle size and a surface area of around 1000 m^2/g. Sigma-Aldrich (USA) supplied magnesium nitrate hexahydrate (CAS# 13446-18-9). Our theoretical investigation used XTB tight-binding semi-empirical quantum chemistry software for geometry optimization, nonbonded interaction site identification, and electrochemical calculations (Bannwarth et al., 2019). Bentonite's 3-D structural file was retrieved from the Crystallography Open Database (code #1100106) (Gražulis et al., 2012). The XTB software was used to optimize the geometry of a Mg nanocluster at the bentonite structure's center.

2.2 Apparatus and measurements

EDX analyses were done using the JSM 6510A scanning electron micrograph module. XRD patterns were taken using a Philips X'Pert-Pro MPD diffractometer at 40 kV, 40 mA, and Cu Kα 1.5418 Å radiation from 5° to 60°. We measured dielectric characteristics and electrical conductivity from 25°C to 120°C and 100 Hz to 1 MHz using the E4990A Impedance Analyzer. No D.C. bias was used, and A.C. amplitude was 0.5 V. We constructed 1 mm-thick, 0.5 cm-radius circular disk (or pellet) samples for impedance measurement. We measured the sample surface temperature with a mercury bulb thermometer on a temperature-controlled hot plate. Estimated dielectric permittivity (ϵ`) comes from:

$$\varepsilon' = Cd/\varepsilon_o A \quad (1)$$

wherein C represents the capacitance, d denotes the sample thickness, ε_o is the free space permittivity, and A represents the area of the measuring electrode on the sample's surface.

The estimated electric modulus is given by $M^* = M' + iM''$ which has a real $M' = \frac{\varepsilon'}{\varepsilon'^2 + \varepsilon''^2}$ and imaginary $M'' = \frac{\varepsilon''}{\varepsilon'^2 + \varepsilon''^2}$ components that are based on the real, ε', and imaginary, ε'', permittivity. To determine AC conductivity, use the formula $\sigma_{ac} = \omega\varepsilon_0\varepsilon' tan\delta$, where $tan\delta$ is the loss tangent, and ω is the angular frequency of the applied A.C. signal from the impedance analyzer. To avoid impedance interference, copper tape electrodes on samples with thin adhesive coverings received the A.C. signal. This method avoided conductive pastes like silver paste, which could cause impedance signals.

2.3 Composite preparation

The Mg/Bento was prepared using the wet impregnation method. Initially, Bento was stirred while adding H_2O. We added a predetermined amount of metal salt to the blend and rapidly swirled it for three hours at room temperature. A powdered composite was obtained by drying the solution at 393 K for 12 hours. Finely grinding the powder produced a smooth texture. A compressor formed circular, disk-like pellets from 0.30 g of fine powder for dielectric measurements. The manuscript uses "Bento" to refer to undoped bentonite, whereas "Mg/Bento" refers to Bento doped with <1% Mg for clarity and consistency.

3. Results and discussion

3.1 Composites characterizations

3.1.1 X-ray diffraction (XRD)

The study examined pure bento with 1% Mg using XRD. Fig. 1 shows pure Bento and Mg/Bento spectra. The Bento contains SiO_2 (S), quartz (Q), and montmorillonite (M) (Salah et al., 2019), with quartz being the most prominent component based on its XRD peaks. Both samples have a SiO_2 diffraction peak at 2θ = 21.52° and montmorillonite peaks at 2θ = 23.6°, 28.16°, and 61.94°. Quartz diffraction peaks were identified at 2θ = 26.72°, 50.11°, 51.16°, 54.17°, and 68.12°. Comparable patterns were found by Salah et al. (2019). The Mg-NPs' XRD pattern is shown in Fig. 1. The XRD spectrum has multiple distinct peaks. Five characteristic peaks were seen in Mg/Bento at 2θ = 30.16°, 32.56°, 36.11°, 43.42°, 57.11°, and 64.34° corresponding to the crystallographic indices (100), (002), (101), (102), (110), and (103), respectively.

The observed peaks align with the data provided in the database (JCPDS 04-0770), verifying that the resulting microspheres consisted of Mg. Furthermore, five peaks were observed at 2θ = 39.76°, 47.39°, 48.67°, 54.97°, and 56.30°, were observed as impurity phase. Their peaks might be related to the Magnesium disilicide (Mg_2Si) as addressed by Xiao et al. (2020) and Yi et al. (2023). Based on the hexagonal Mg structure (Walker and Marezio, 1959), the lattice parameters (a, c) of

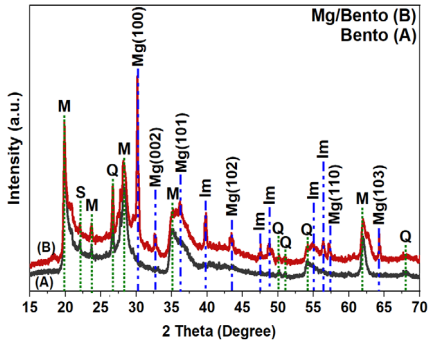

Fig. 1. XRD intensities of bentonite (Bento) and Mg/Bento composites with SiO_2 (S), Quartz (Q), Magnesium (Mg), Montmorillonite (M), and impurities (Im).

Mg nanoparticles were computed (Karyaoui et al., 2015). Where 'd' is interplanar distance and 'h', 'k', and 'l' are Miller indices.

$$\frac{1}{d_{hkl}^2} = \frac{4}{3}\left[\frac{h^2 + hk + k^2}{a^2}\right] + \frac{l^2}{c^2} \quad (2)$$

The values obtained for a, and c were 2.71 Å and 5.50 Å, respectively. This calculation uses first order Brag reflections at 2θ = 30.16°, and 36.12° for the Mg XRD intensities with (100) and (101) indices shown in Fig. 1. The average grain size (D) was calculated to be approximately 7 nm and 15 nm for Bento and Mg/Bento respectively, from the Debye - Scherrer's equation (Patterson, 1939).

$$D = 0.94\lambda/\beta\cos\theta \quad (3)$$

where λ is the incident CuKα radiation wavelength, β is full width at half maximum (FWHM) of the respective peak and θ represents the diffraction peak angle. Thus, the XRD profile in Fig. 1 confirmed the existence of Mg nanocrystals, demonstrating that the technique utilized in this work successfully prepared the Mg nanoparticles.

3.2 SEM results

The surface morphology of uncoated and magnesium-coated bentonite adsorbents was examined using SEM. Fig. 2 illustrates the SEM images of uncoated bentonite (a) and Mg/Bento (b). The uncoated bentonite displays large pores with varied sizes, shapes, and distributions across its surface. These pores provide insight into bentonite's natural texture and structure, highlighting its high surface area and irregular pore distribution. In contrast, the Mg/Bento composite shows a significantly altered surface morphology. The SEM images reveal a flaky configuration with noticeable irregular agglomerations within the bentonite matrix. The Mg/Bento particles are substantially less agglomerated compared to the uncoated bentonite sample. Some larger particles are present, seemingly formed by the aggregation or overlapping of smaller ones.

This observation suggests that the magnesium coating process affects the particle size distribution within the composite, leading to a mixture of particle sizes and shapes. The irregular morphology and varied particle sizes in the Mg/Bento composite complicate the determination of precise particle dimensions in the SEM images. The agglomerated nature of the composite makes it challenging to measure individual particle sizes accurately.

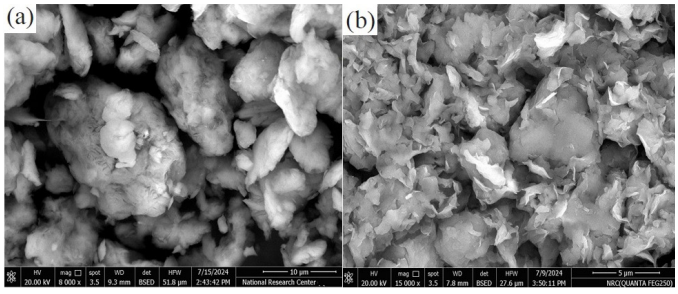

Fig. 2. SEM micrographs of (a) Bento and (b) Mg/Bento. SEM: Scanning electron microscope.

3.3 EDX results

An XRD spectrometer analyzed pure bentonite and Mg/bento composite element compositions (Fig. 3). The figure demonstrates that pure bentonite has a lot of O, Si, C, Al, and little Fe, Mg, N, Na, and Ca. Salah et al., (2019) and Özcan et al. (2009) reported similar findings. It contained O, Si, C, Al, Ca, Fe, Mn, Na, S, N, Cl, and Mg. Mg/Bento's EDX spectra show a peak for Mg, among other elements, indicating good growth.

3.4 Dielectric properties

We investigated the dielectric properties of Bento and Mg/Bento composites over a frequency range of up to 1 MHz and temperatures from 25°C to 120°C.

The frequency-dependent permittivity (E') of both Bento and Mg/Bento was measured at various temperatures. In this frequency range, both materials exhibited a monotonic decrease in permittivity with increasing frequency at all temperatures, as illustrated in Fig. 4. The inability of the material's dipoles to quickly realign with the alternating electric field as the frequency increases causes this decrease in permittivity with rising frequency. As a result, the overall polarization of the material diminishes, leading to a reduction in dielectric permittivity, particularly at lower frequencies. This behavior is consistent in both pure bentonite and Mg-incorporated bentonite samples. We observe that the permittivity of Mg/Bento is lower than that of pure bentonite at lower temperatures (below 50°C), suggesting that the incorporation of Mg nanoparticles initially reduces polarization. However, as the temperature increases, the dielectric constant of Mg/Bento shows a pronounced rise, particularly at higher frequencies.

Temperature significantly influences the dielectric properties of Mg/Bento, causing Mg/Bento to exhibit more substantial changes in permittivity compared to pure bentonite as the temperature increases. The Maxwell-Wagner interfacial polarization effect, prominent in heterogeneous materials like Mg/Bento, explains this behavior. At lower frequencies, charge carriers accumulate at the interfaces between the Mg nanoparticles and the bentonite matrix, enhancing polarization.

As temperature increases, the mobility of these charge carriers also increases, leading to a more significant polarization effect at the interfaces, resulting in a higher dielectric constant. The data demonstrate that at elevated temperatures, the permittivity of Mg/Bento surpasses that of pure bentonite, highlighting the enhanced Maxwell-Wagner interfacial polarization due to the presence of Mg nanoparticles, which introduce additional interfaces that amplify this effect (Ellison et al., 2018). On the other hand, Fig. 5 shows the dielectric loss (E") of Bento and Mg nanoparticles supported on bentonite (Mg/Bento) as a function of frequency at various temperatures. Fig. 5 presents the dielectric loss (E") of Bento and Mg/Bento as a function of frequency at various

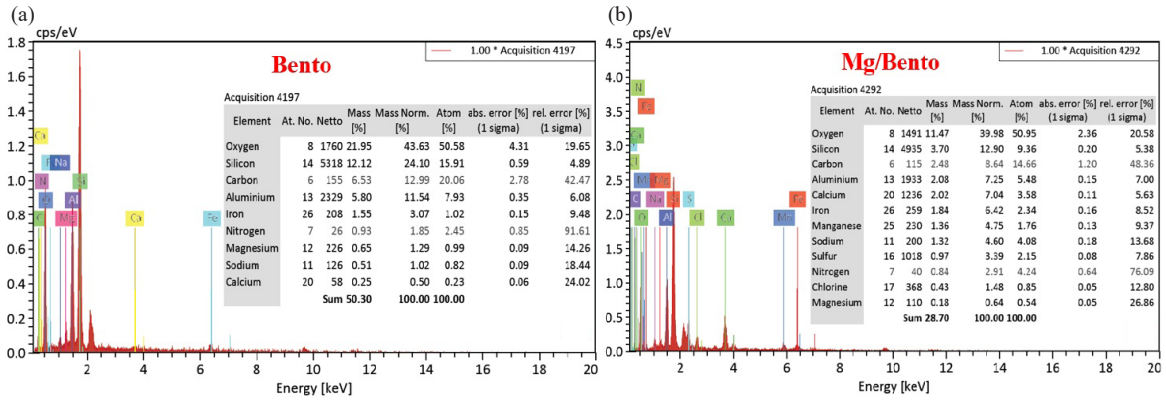

Fig. 3. The EDX results for undoped (a) Bento and (b) Mg/Bento. EDX: Energy-Dispersive X-ray.

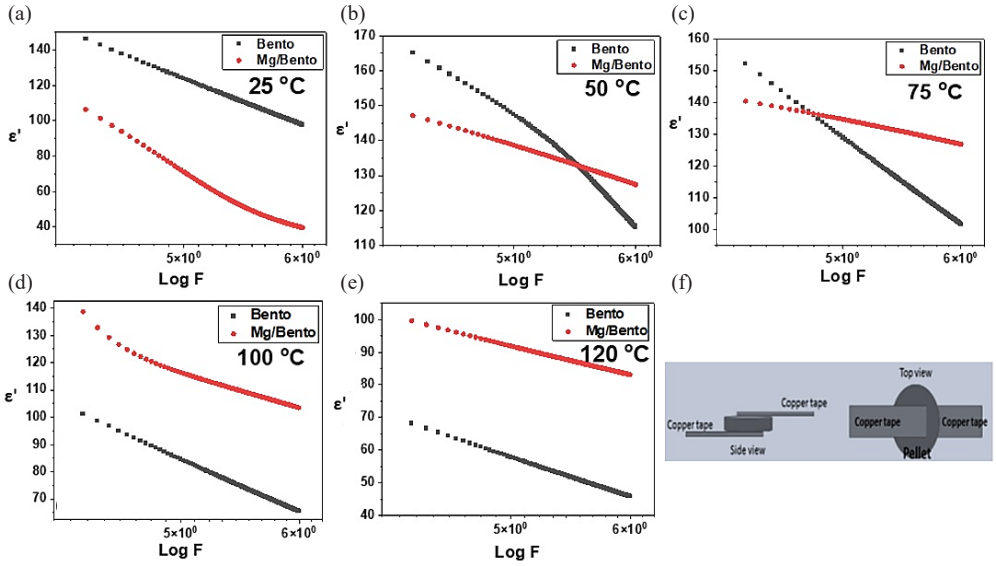

Fig. 4. Variations in the permittivity of Bento and Mg/Bento samples over different frequencies at (a) 25°C, (b) 50°C, (c) 75°C, (d) 100°C, and (e) 120°C, (f) illustrates the sample pellet equipped with copper connectors utilized for data collection.

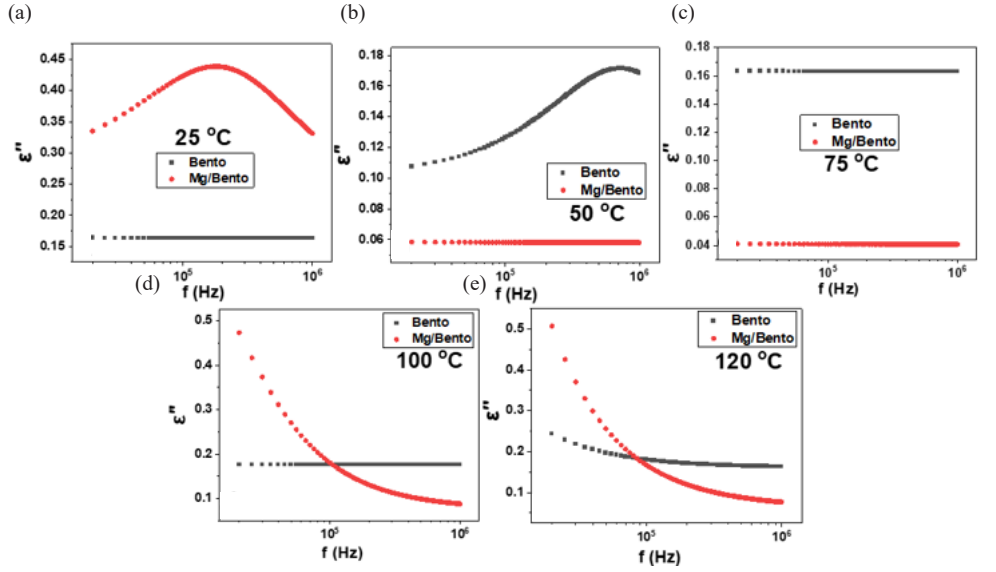

Fig. 5. Dielectric loss changes of pure Bento and Mg-incorporated Bento at different frequencies at (a) 25°C, (b) 50°C, (c) 75°C, (d) 100°C, and (e) 120°C.

temperatures. At 25°C, Mg/Bento exhibits a higher dielectric loss than pure bentonite, indicating that incorporating Mg nanoparticles enhances energy dissipation mechanisms, potentially due to increased electrical conductivity or more active dipole relaxation processes.

As temperature increases, the dielectric loss of bentonite exceeds that of Mg/Bento, with this difference becoming more pronounced at higher temperatures, except in certain low-frequency regions. In other words, Mg/Bento exhibits a lower dielectric loss at high temperatures due to the stabilizing influence of Mg nanoparticles, which improve charge transport while reducing energy dissipation.

This enhancement arises from the interfacial polarization facilitated by Mg, which allows for more efficient charge alignment, thus improving dielectric stability at high temperatures. The variation in dielectric loss with temperature can better be understood with the permittivity data (E') presented in Fig. 4. The monotonic decrease in permittivity (E') with increasing frequencies for both samples suggests reduced dipolar alignment at higher frequencies. While Mg/Bento exhibits lower permittivity than bentonite at low temperatures, the permittivity of Mg/Bento significantly increases with temperature, especially at higher frequencies, due to enhanced charge carrier mobility and Maxwell-Wagner interfacial polarization. We emphasize that the observed increase in permittivity for Mg/Bentonite at elevated frequencies can be attributed primarily to Maxwell-Wagner polarization. Nevertheless, the dispersion of magnesium nanoparticles within the bentonite matrix could act as an additional contributing factor, as it introduces extra charge-trapping sites that enhance the overall dielectric response. This increase in polarization at elevated temperatures corresponds to the observed decrease in dielectric loss for Mg/Bento, indicating that although permittivity increases due to improved dipole alignment or charge accumulation, energy dissipation (E'') is more controlled in Mg/Bento compared to Bento. This relationship between E' and E'' highlights the impact of temperature and frequency on the dielectric behavior of these materials, with Mg/Bento exhibiting distinct characteristics due to the presence of Mg nanoparticles. Therefore, Mg doping significantly enhances bentonite's dielectric properties by promoting interfacial polarization and establishing conductive pathways within the composite structure. The integration of Mg nanoparticles enhances permittivity by increasing the mobility of charge carriers, especially at higher temperatures, thus strengthening the dielectric response.

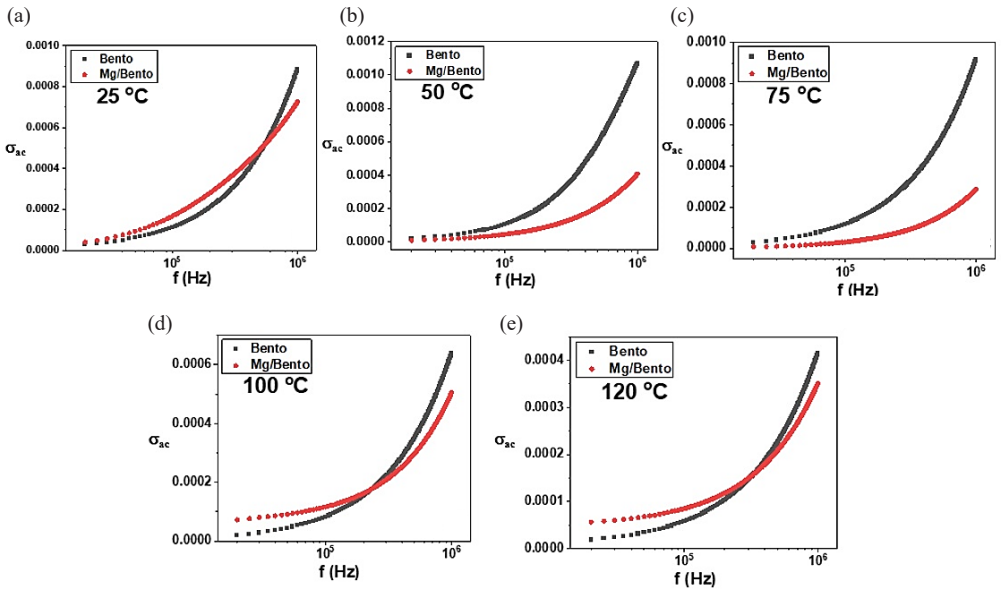

Fig. 6. Conductivity variation of Bento and Mg-incorporated Bento samples as a function of frequency at (a) 25, (b) 50, (c) 75, (d) 100, and (e) 120°C.

3.4.1 Ac conductivity (σ_{ac})

Understanding the conductivity of materials is crucial to investigating the impact of Mg/Bento. In Fig. 6, the electrical conductivity as a function of frequency is illustrated for both Bento and Mg/Bento across various temperatures. In general, the rate of electrical conductivity increases exponentially with frequencies, while the conductivity generally increases with increasing temperature (although there is a slight mismatch at 120°C) (Essaleh et al., 2023).

Fig. 6 illustrates the exponential increase in electrical conductivity with frequency across various temperatures for both bentonite and Mg/Bento. The powers law dependence of conductivity describes how the frequency of the applied electric field influences the movement of charge carriers and explains this behavior. The charge carriers gain more energy at higher frequencies, allowing them to move more freely and contribute to higher conductivity. The power law dependence of the conductivity on frequency typically represents this relationship, with the frequency exponent reflecting the material's response. In our case, the exponent at high frequency is around one, suggesting some variable range hopping conduction between localized sites such as the Mg nanoparticles. Incorporating Mg nanoparticles establishes new conductive pathways within the bentonite matrix, facilitating charge carrier flow. These pathways reduce the resistance to charge movement, as the Mg nanoparticles act as conductive fillers that bridge charge gaps in the matrix, enhancing overall conductivity. Furthermore, Mg nanoparticles create more interfaces within the bentonite matrix, serving as sites for improved charge carrier movement. These interfaces decrease barriers to charge mobility, facilitating faster charge migration. Conductivity typically increases with temperature, as elevated temperatures supply additional energy to charge carriers, thereby improving their mobility. The activation energy for charge carriers in Mg/Bento composites is lower than that in pure bentonite. Incorporating magnesium nanoparticles reduces the energy barrier for charge mobility by establishing conductive pathways. This enhancement in conductivity is temperature-dependent, thereby improving overall electrical performance. Fig. 6 depicts the conductivity, while Fig. 5 illustrates the dielectric loss. The Mg/Bento composite and pure bentonite demonstrate a frequency-dependent dielectric loss. However, Mg/Bento exhibits lower dielectric loss at elevated temperatures than pure bentonite. This is likely due to the presence of magnesium, which enhances charge transport, resulting in higher conductivity with reduced energy loss. Additionally, magnesium nanoparticles may decrease resistive impedance by improving charge mobility. However, the data exhibits some irregularity at 120°C, which could be attributed to structural changes or other temperature-dependent factors that influence the charge carrier dynamics differently at this temperature.

It is worth stressing that the incorporation of magnesium nanoparticles significantly enhances the temperature-dependent conductivity of the Mg/bentonite composite compared to pure bentonite. This improvement stems from better charge transport mechanisms and reduced activation energy for carrier mobility. The Mg nanoparticles create additional pathways for charge conduction, lowering energy barriers for hopping or tunneling between localized states. Moreover, they likely increase polarization at the composite interfaces, aligning with the Maxwell-Wagner polarization model, which suggests that charge accumulation occurs at these interfaces. As thermal energy rises, charge carrier mobility improves, enhancing conductivity. In contrast, pure bentonite has limited conductivity due to fewer conduction pathways and higher activation energy for charge transport.

3.4.2 The electric modulus

The electric modulus behavior (real, M′, and imaginary, M″) offers insights into the relaxation dynamics and conduction mechanisms of materials. The real component of the electric modulus, M′, typically exhibits an increase in frequency for both Bento and Mg/Bento. Fig. 7 illustrates that an increase in frequency results in a decrease in dielectric permittivity, which corresponds to the observed rise in M′.

Fig. 8 shows the imaginary electric modulus M″ versus frequency for Mg/Bento samples. The data reveals a trend where M″ decreases as temperature rises, with a notable convergence toward zero at lower frequencies. This trend signifies the elimination of electrode polarization in the samples due to the thermally activated nature of the dielectric constant. Moreover, M" increases with frequency for both samples, likely forming a broad peak at higher frequencies. This behavior suggests a relaxation process associated with charge movement, particularly at the interface between the Mg nanoparticles and the bentonite. This interface polarization is more significant for Mg/Bento samples, making the peak structure more noticeable compared to pure Bento. The broad peak observed in the imaginary modulus of Mg/Bento at higher frequencies may be linked to a relaxation mechanism, particularly charge carrier hopping. Mg nanoparticles enhance this hopping mechanism by generating conductive sites that facilitate the movement of charges. As a result, this relaxation process becomes more pronounced compared to pure bentonite. As the temperature rises, M" values for both samples become more spread out, suggesting that the relaxation processes are more temperature-dependent, causing increased variation in the charge dynamics (Alotaibi et al., 2020).

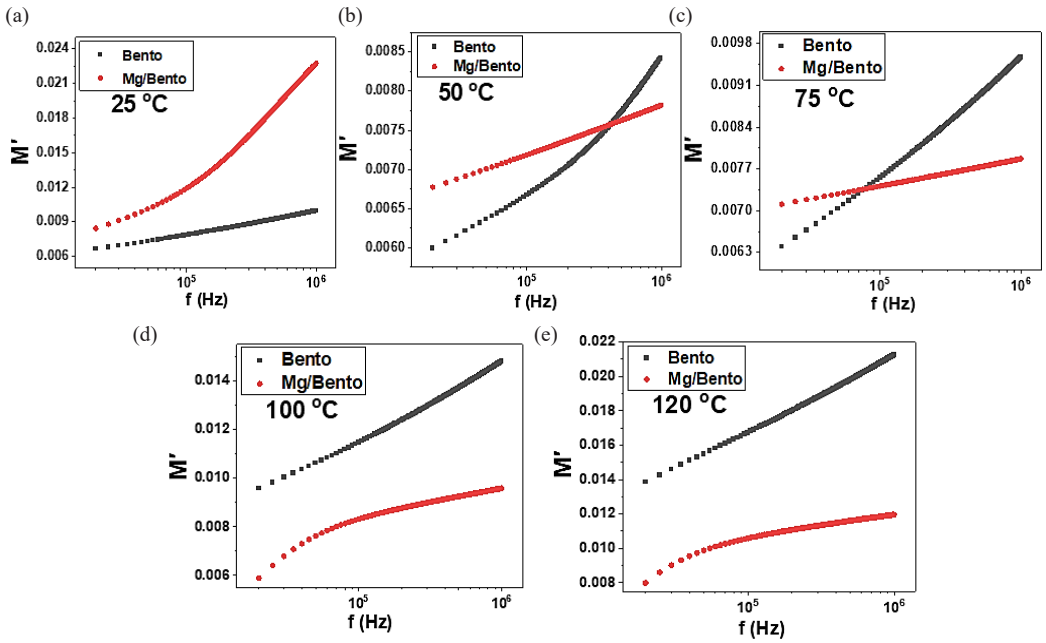

Fig.7. Depicts the variations in the real component of the electric modulus for both Bento and Mg-incorporated Bento samples over various frequencies and temperatures: (a) 25°C, (b) 50°C, (c) 75°C, (d) 100°C, and (e) 120°C.

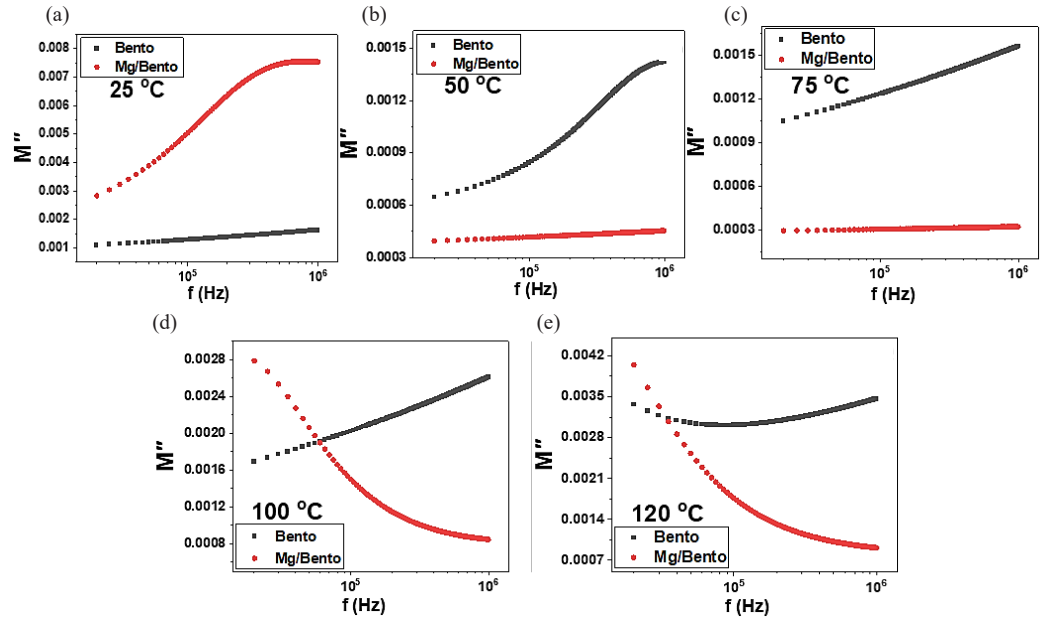

Fig. 8. Illustrates the changes in the imaginary component of the electric modulus for pure Bento and Mg/Bento specimens across various frequencies and temperatures: (a) 25°C, (b) 50°C, (c) 75°C, (d) 100°C, and (e) 120°C.

3.5 Tight binding calculation

The evaluation of the energies associated with HOMO and LUMO enables accurate predictions in the examination of charge transfer, chemical reactivity, bioactivity, and compound stability (Abdel-Baset and Hassen 2016). Fig. 9 presents the iso-surfaces of the HOMO and LUMO for both the Bento and the Mg/Bento compounds, derived from their geometrically optimized structures. The localization of LUMO within the nanoclusters of the Mg/Bento structure could suggest its chemical stability. According to Table 1, the calculated HOMO energy level for pure bentonite is -10.4376 eV. The HOMO energy level for Mg/Bento exhibits a modest increase, reaching -9.1189 eV.

In assessing kinetic stability, the HOMO-LUMO energy gap ($E_{LUMO} - E_{HOMO}$) serves as a valuable metric, with E_{HOMO} and E_{LUMO} denoting the energies of the highest occupied molecular orbital and the lowest unoccupied molecular orbital, respectively.

An increased energy gap signifies that a greater amount of energy is necessary for the excitation of electrons. The comparison of energy gaps between Bento and Mg/Bento reveals that the introduction of Mg has resulted in a reduction of the band gap of Bento (1.6260 eV), which may have implications for its conductivity and electronic characteristics. Significantly, the Mg/Bento exhibits an energy gap of 0.4312 eV, indicating its promising potential for applications in conductivity. Chemical hardness, defined as $\eta = -(E_{HOMO} - E_{LUMO})/2$, serves as a significant parameter that indicates a structure's resilience against deformation. An increased HOMO-LUMO energy gap signifies enhanced hardness, reflecting superior stability and greater resistance to alterations in electronic distribution or polarization. Table 1 indicates a reduction in the chemical hardness of Mg/Bento to 0.2156 eV in comparison to that of Bento, implying diminished stability and an increased tendency to accept electrons. Moreover, the negative binding

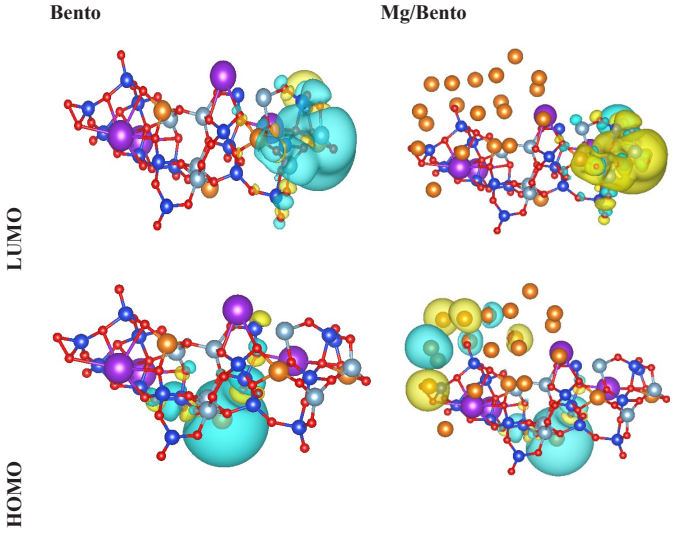

Fig. 9. The geometrically optimized Bento (left panels) and Mg/Bento (right panels) structures. The HOMO and LUMO iso-surfaces (yellow and blue iso-surfaces with -0.01 and 0.01 au levels, respectively). HOMO: Highest occupied molecular orbital, LUMO: Lowest unoccupied molecular orbital.

Table 1.
The calculated energy values of the HOMO and LUMO orbitals, along with other electronic parameters, for both Bento and Mg/Bento.

	Bento	Mg/Bento
HOMO (eV)	-10.4376	-9.1189
LUMO (eV)	-8.8116	-8.6876
Energy gap (eV)	1.6260	0.4312
Chemical hardness (eV)	0.813	0.2156
Binding energy (eV)	-	-7.5623

HOMO: Highest occupied molecular orbital, LUMO: Lowest unoccupied molecular orbital, Bento: bentonite, Mg: Magnesium.

energy observed in the Mg/Bento samples substantiates the stability of the Mg nanocomposites on the Bento surface.

3.6 Charge-density analysis

The charge density difference method is a crucial tool for elucidating the electronic interactions at the interface of nanocluster-supported systems. By providing detailed insights into the redistribution of electronic charge, this method helps understand how interfacial phenomena influence the overall properties of the composite material. This approach is particularly relevant in the context of Mg nanoclusters supported on Bento, where nonbonding interactions play a significant role. The Maxwell–Wagner effect effectively explains the pronounced dependence of dielectric permittivity on frequency, as revealed by experimental dielectric measurements of the Mg/Bento system (Barsoukov and MacDonald 2018). The charge density difference analysis provides a deeper understanding of this phenomenon. The calculated charge density difference reveals a significant accumulation of negative charge at the interface between the Mg nanocluster and the Bento, as illustrated in Fig. 10. The Maxwell–Wagner effect explains this concentration of negative charge density, which is consistent with the experimental findings. The nonbonding nature of the interaction between the Mg nanocluster and the Bento surface suggests that the charge redistribution is primarily due to electrostatic interactions and polarization effects rather than chemical bonding. The Bento surface, composed of Si-O tetrahedral and Al-O octahedral sheets, interacts with the Mg nanocluster through van der Waals forces and electrostatic interactions.

These nonbonding interactions lead to electronic charge redistribution, with negative charge density concentrating at the interface. This interfacial charge accumulation enhances the interfacial polarization, contributing significantly to the dielectric relaxation observed experimentally.The agreement between the theoretical charge density distribution and the experimental dielectric measurements underscores the importance of considering interfacial effects in understanding the dielectric properties of nanocluster-supported

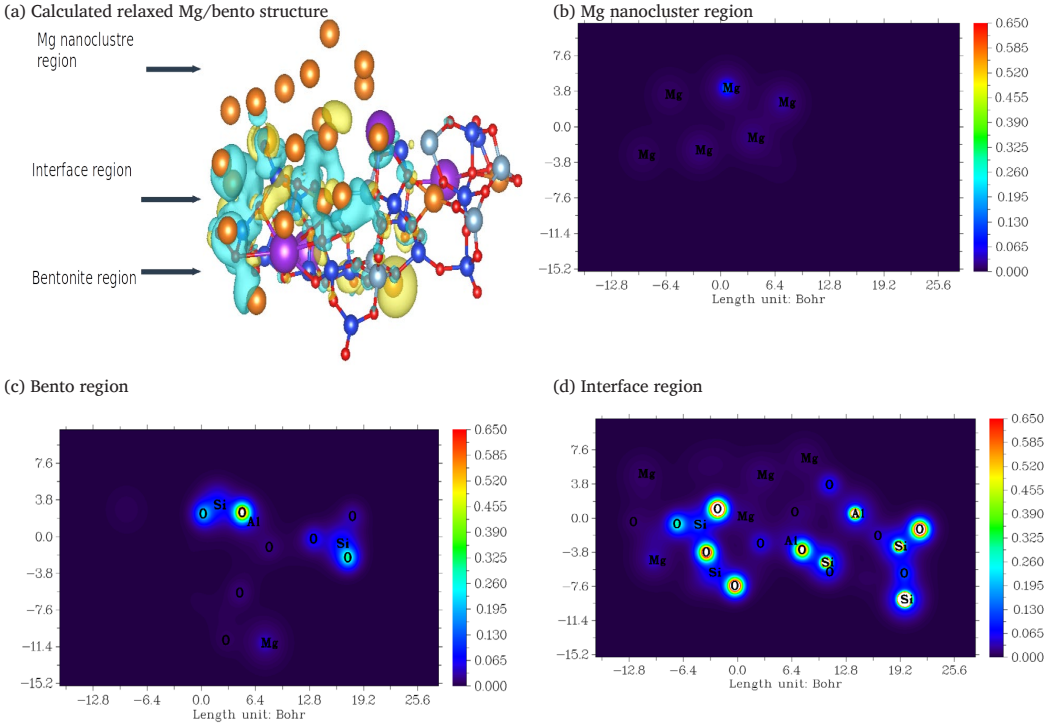

Fig. 10. (a) Calculated relaxed Mg/Bento structure. Charge density 2D plots across the (b) Mg nanocluster region, (c) the Bento region, and (d) the Mg-Bento interface region.

systems. As shown in Fig. 8, the charge density difference method highlights the concentration of negative charge density at the Mg nanocluster-Bento interface, consistent with the experimental dielectric data explained by the Maxwell–Wagner effect. This finding underscores the importance of interfacial charge in determining the dielectric properties.

It suggests that nonbonding interactions play a crucial role in the electronic behavior of the Mg/Bento system. Understanding these interfacial phenomena is essential for designing and applying nanocomposites with tailored electronic and dielectric properties.

4. Conclusion

This study investigates the structural, morphological, and dielectric enhancements introduced by magnesium doping in bentonite composites. Incorporating Mg nanoclusters significantly improved bentonite's dielectric and electronic properties. X-ray diffraction analysis confirmed the successful Mg integration, with characteristic Mg peaks at 2θ values of 30.16°, 32.56°, and 36.11°. This doping increased the average grain size from 7 nm in pure bentonite to 15 nm in Mg/Bento, a structural shift that supports enhanced charge transport pathways. Dielectric measurements revealed that Mg/Bento exhibits a substantial increase in permittivity at higher temperatures and frequencies, attributed to Maxwell-Wagner interfacial polarization, with permittivity notably increasing as temperature rises. Furthermore, theoretical calculations, including tight-binding analysis, demonstrated a reduced HOMO-LUMO energy gap from 1.6260 eV in pure bentonite to 0.4312 eV in Mg/Bento, indicating a considerable improvement in conductivity and potential for electronic applications. The charge density analysis confirmed significant charge accumulation at the Mg/bentonite interface, enhancing dielectric response and conductivity. These findings underscore the novelty of Mg doping as a strategy to boost bentonite's dielectric and electronic properties, opening avenues for applications in environmental remediation, catalysis, and advanced electronic materials where high permittivity and improved charge transport are advantageous. This research highlights Mg/Bento as a promising material with structural and electronic advancements suitable for applications in environmental remediation and electronic devices, where enhanced dielectric properties and conductivity are critical.

CRediT authorship contribution statement

Abdulaziz Almalki: Conceptualization, methodology, validation, formal analysis, investigation, data curation, writing—original draft, writing—review & editing, supervision. **Talat H. Habeeb:** Software, writing—original draft, writing—review & editing, visualization.

Ali H. Bashal: Conceptualization, methodology, validation, formal analysis, investigation, data curation, writing—original draft, writing—review & editing, supervision. **Hussam Y. Alharbi:** Methodology, software, writing—original draft, writing—review & editing.

Data availability statement

Data will be available by request.

Declaration of competing interest

The authors declare that they have no known competing financial interests or personal relationships that could have appeared to influence the work reported in this paper.

Declaration of Generative AI and AI-assisted technologies in the writing process

The authors confirm that there was no use of artificial intelligence (AI)-assisted technology for assisting in the writing or editing of the manuscript and no images were manipulated using AI.

References

Abdel-Baset, T.A., Hassen, A., 2016. Dielectric relaxation analysis and ac conductivity of polyvinyl alcohol/polyacrylonitrile film. Physica B: Condensed Matter 499, 24-28. https://doi.org/10.1016/j.physb.2016.07.002

Abou Elfadl, A., Bashal, A.H., Althobaiti, M.G., 2022. A study on dielectric permittivity, structure, and AC conductivity of zinc and copper doped bentonite composites. J. Inorg. Organomet. Polym. 32, 191-199. https://doi.org/10.1007/s10904-021-02112-z

Alotaibi, A.A., Abdel-Baset, T., Bashal, A.H., 2020. Structural, dielectric and electrical characterization of (Co) x (Ni/bentonite) composites. J. Taibah Univ. Sci. 14, 1193–1200.

Bannwarth, C., Ehlert, S., Grimme, S., 2019. GFN2-xTB—An accurate and broadly parametrized self-consistent tight-binding quantum chemical method with multipole electrostatics and density-dependent dispersion contributions. J. Chem. Theory Comput. 15, 1652-1671. https://doi.org/10.1021/acs.jctc.8b01176

Barsoukov, E., MacDonald, J.R., 2018. Impedance spectroscopy: Theory, experiment, and applications. John Wiley & Sons.

Bashal, A.H., 2024. Tailoring the dielectric properties of bentonite for advanced capacitor applications: The role of ruthenium and strontium incorporation. J. Saudi Chem. Soc. 28, 101874. https://doi.org/10.1016/j.jscs.2024.101874

Bashal, A.H., Saad, M.H., Khalafalla, M.A.H., 2020. The effect of nickel percentage on the dielectric properties of bentonite. Journal of Taibah University for Science 14, 496-499. https://doi.org/10.1080/16583655.2020.1747216

Borah, D., Nath, H., Saikia, H., 2022. Modification of bentonite clay & its applications: A review. Rev. Inorg. Chem. 42, 265–282.

Ellison, C., McKeown, M.S., Trabelsi, S., Marculescu, C., Boldor, D., 2018. Dielectric characterization of bentonite clay at various moisture contents and with mixtures of biomass in the microwave spectrum. J. Microw. Power Electromagn. Energy 52, 3-15. https://doi.org/10.1080/08327823.2017.1421407

Essaleh, M., Bouferra, R., Kadiri, I., Belhouideg, S., Mansori, M., Bouchehma, A., Oubani, M., Benjelloun, M., 2023. Geotechnical and thermal analysis and complex impedance spectroscopy characterization of pure moroccan bentonite material for civil engineering applications. Eureka: PE, 152-164. https://doi.org/10.21303/2461-4262.2023.002571

Gražulis, S., Daškevič, A., Merkys, A., Chateigner, D., Lutterotti, L., Quirós, M., Serebryanaya, N.R., Moeck, P., Downs, R.T., Le Bail, A., 2012. Crystallography open database (COD): An open-access collection of crystal structures and platform for world-wide collaboration. Nucleic Acids Res. 40, D420–D427.

Jiang, S.P., 2006. A review of wet impregnation—An alternative method for the fabrication of high performance and nano-structured electrodes of solid oxide fuel cells. Mater. Sci. Eng. A 418, 199-210.

Karyaoui, M., Mhamdi, A., Kaouach, H., Labidi, A., Boukhachem, A., Boubaker, K., Amlouk, M., Chtourou, R., 2015. Some physical investigations on silver-doped znO sprayed thin films. Materials Science in Semiconductor Processing 30, 255-262. https://doi.org/10.1016/j.mssp.2014.09.017

Mehrabadi, B.A.T., Eskandari, S., Khan, U., White, R.D., Regalbuto, J.R. 2017. Chapter one - A review of preparation methods for supported metal catalysts. In: Chunshan, S., editor, Advances in Catalysis, Vol. 61, Academic Press, pp. 1-35. Available from: https://doi.org/10.1016/bs.acat.2017.10.001

Mutahir, S., Yaqoob, F., Khan, M.A., Alsuhaibani, A.M., Abouzied, A.S., Refat, M.S., Huwaimel, B., 2023. Schiff-based modified bentonite clay composites for wastewater treatment: Experimental and DFT-based analysis. Crystals 13, 806. https://doi.org/10.3390/cryst13050806

Neelamma, M.K., Holla, S.R., Selvakumar, M., Chandran, P.A., De, S., 2022. Bentonite clay liquid crystals for high-performance supercapacitors. J. Electron. Mater. 51, 2192-2202. https://doi.org/10.1007/s11664-022-09469-y

Ozcan, A., Gök, O., Ozcan, A., 2009. Adsorption of lead(II) ions onto 8-hydroxy quinoline-immobilized bentonite. J. Hazard. Mater. 161, 499-509. https://doi.org/10.1016/j.jhazmat.2008.04.002

Patterson, A.L., 1939. The diffraction of x-rays by small crystalline particles. Phys. Rev. 56, 972-977. https://doi.org/10.1103/physrev.56.972

Prasad, S.V.S., Prasad, S.B., Verma, K., Mishra, R.K., Kumar, V., Singh, S., 2022. The role and significance of magnesium in modern day research-A review. J. Magnesium Alloys 10, 1-61. https://doi.org/10.1016/j.jma.2021.05.012

Salah, A.B., Gaber, S.M., T. Kandil, A.h., 2019. The removal of uranium and thorium from their aqueous solutions by 8-hydroxyquinoline immobilized bentonite. Minerals 9, 626. https://doi.org/10.3390/min9100626

Sekunowo, O.I., Durowaye, S.I., Lawal, G.I., 2015. An overview of nano-particles effect on mechanical properties of composites. Int. J. Mech. Aerosp. Ind. Mechatron. Manuf. Eng., 9, 1, 1–7.

Walker, G.B., Marezio, M., 1959. Lattice parameters and zone overlap in solid solutions of lead in magnesium. Acta Metallurgica 7, 769-773. https://doi.org/10.1016/0001-6160(59)90090-2

Xiao, P., Gao, Y., Yang, S., Li, Y., Zhao, S., Liu, Q., 2020. Investigations on microstructure, mechanical properties and tribological behavior of in-situ Mg2Si particles reinforced AZ91 composites. Mater. Res. Express, 6, p. 1265f8.

Yi, Z., Shan, Z., Fang, L., Lu, C., Xu, Z., 2023. Enhanced photostability of chlorophyll by introducing Mg2Si as an O2-depleting agent. J. Mater. Sci. 58, 6281-6296. https://doi.org/10.1007/s10853-023-08398-3

Zaki, A.A., Bashal, A.H., Abdel-Basset, T.A., 2023. Characterization and investigation of the effect of bimetallic dopants (Zn-Ni and hg-Ni) on the dielectric, ac conductivity and optical properties of tiO2. Arab. J. Sci. Eng. 48, 8103-8114. https://doi.org/10.1007/s13369-022-07468-z